STAR Protocols

CellPress
OPEN ACCESS

Protocol

Quantification of autophagy flux in isolated mouse skeletal muscle fibers with overexpression of fluorescent protein mCherry-EGFP-LC3

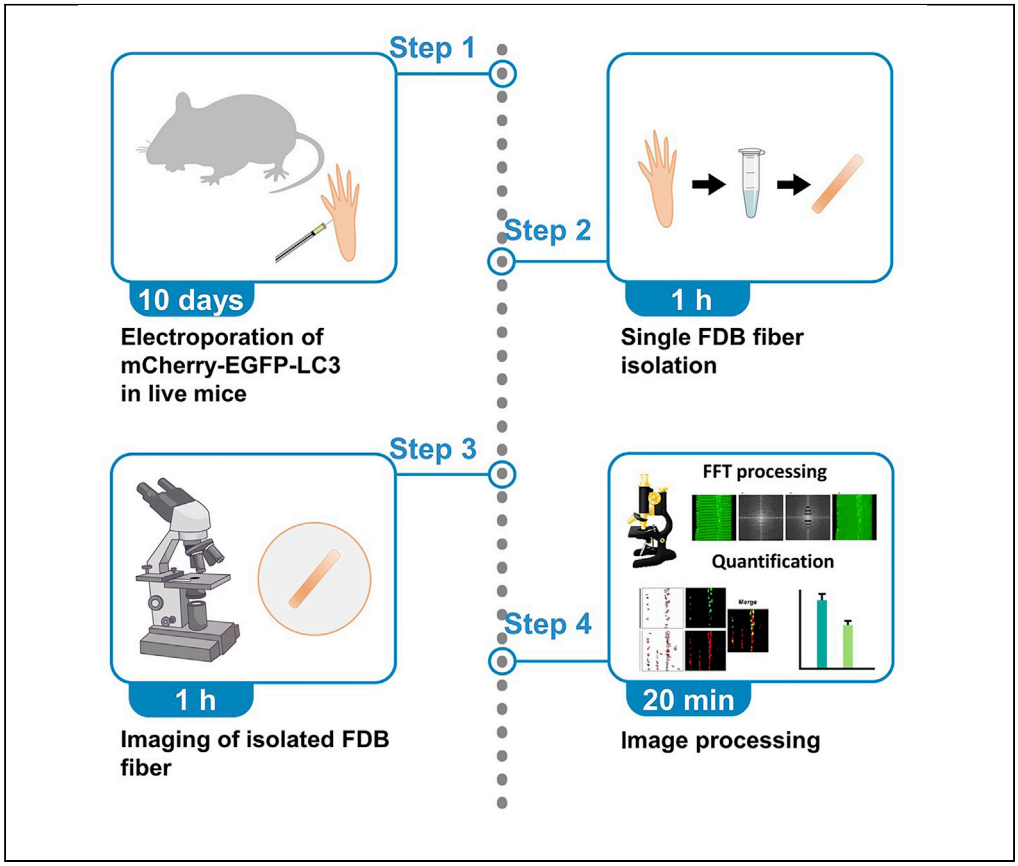

Evaluation of autophagy flux could be challenging for muscle fibers due to the baseline expression of mCherry-EGFP-LC3 along the Z-line. We established a protocol to overcome this difficulty. We overexpress mChery-EGFP-LC3 in the FDB muscle of an adult mouse via electroporation. Then, we enzymatically digest FDB muscle to yield individual fibers for live cell imaging. Finally, we develop an ImageJ-based program to eliminate the baseline striation pattern and semi-automatically quantify autophagosomes (APs) and autolysosomes (ALs) for autophagy flux analysis.

Publisher's note: Undertaking any experimental protocol requires adherence to local institutional guidelines for laboratory safety and ethics.

Xinyu Zhou, Ju Hwan Cho, Jianxun Yi, ..., Jingsong Zhou, Jae-Kyun Ko, Jianjie Ma

xinyu.zhou@osumc.edu (X.Z.)
jingsong.zhou@uta.edu (J.Z.)
jae-kyun.ko@osumc.edu (J.-K.K.)

Highlights

mCherry-EGFP-LC3 is expressed in skeletal muscle for monitoring autophagy activity

Autophagosomes and autolysosomes in isolated muscle fibers are recorded by live cell imaging

FFT based semi-automatic image processing for quantitative evaluation of autophagy flux

Zhou et al., STAR Protocols 4, 101871
March 17, 2023
https://doi.org/10.1016/j.xpro.2022.101871

STAR Protocols

CellPress
OPEN ACCESS

Protocol

Quantification of autophagy flux in isolated mouse skeletal muscle fibers with overexpression of fluorescent protein mCherry-EGFP-LC3

Xinyu Zhou,[1,3,4,*] Ju Hwan Cho,[1,3] Jianxun Yi,[2] Kyounghan Choi,[1] Ki Ho Park,[1] Hua Zhu,[1] Chuanxi Cai,[1] Erin Haggard,[1] Jingsong Zhou,[2,*] Jae-Kyun Ko,[1,5,*] and Jianjie Ma[1]

[1]Department of Surgery, The Ohio State University Wexner Medical Center, Columbus, OH 43210, USA

[2]Department of Kinesiology, University of Texas at Arlington, Arlington, TX 76109, USA

[3]These authors contributed equally

[4]Technical contact

[5]Lead contact

*Correspondence: xinyu.zhou@osumc.edu (X.Z.), jingsong.zhou@uta.edu (J.Z.), jae-kyun.ko@osumc.edu (J.-K.K.)
https://doi.org/10.1016/j.xpro.2022.101871

SUMMARY

Evaluation of autophagy flux could be challenging for muscle fibers due to the baseline expression of mCherry-EGFP-LC3 along the Z-line. We established a protocol to overcome this difficulty. We overexpress mChery-EGFP-LC3 in the FDB muscle of an adult mouse via electroporation. Then, we enzymatically digest FDB muscle to yield individual fibers for live cell imaging. Finally, we develop an ImageJ-based program to eliminate the baseline striation pattern and semi-automatically quantify autophagosomes (APs) and autolysosomes (ALs) for autophagy flux analysis.

BEFORE YOU BEGIN

GFP-LC3 has been used as a fluorescent marker for autophagosomes (AP) in live cell imaging.[1] However, it is not suitable for monitoring autolysosomes (AL) since GFP possesses pKa of 5.9 and is quenched in the acidic compartment.[2] On the contrary, the mCherry protein is relatively stable and remains fluorescent within lysosomes due to its pKa of 4.5.[3] Using this differential sensitivity to lysosomal acidity, imaging of the mCherry-EGFP-LC3 protein can be used to visualize the transition from neutral AP to acidic AL in a cel.[4] While this tandem repeat fluorescent marker has been widely used in imaging of cultured cells, the quantification of AP and AL in skeletal muscle is challenging due to the fact that overexpressed fluorescent LC3 proteins also target to Z-disc in muscle fibers and form a striation pattern of the baseline fluorescence,[5] which presents a challenge in using GFP or RFP fluorescence to quantify AP or AL in muscle fibers. Currently, there is no method to quantify the dynamic process of autophagic execution in isolated skeletal muscle fibers. Our laboratory has routinely used electroporation to express cDNA plasmids in muscle fibers of live mice.[6–9] Here, using electroporation, we expressed mCherry-EGFP-LC3 in the flexor digitorum brevis (FDB) muscle of mice to investigate the autophagy activity in isolated individual muscle fibers. We also obtained the CAG-RFP-EGFP-LC3 transgenic mouse[10,11] from the Jackson Lab (Stock #027139). We found that under starvation conditions, which activate autophagy systematically, the fluorescent patterns of AP and AL are similar between the electroporated FDB fibers and those derived from the transgenic mice (Figure 1). We developed an image analysis protocol to semi-automatically quantify RFP-, GFP- or both positive vesicles from confocal images of isolated skeletal muscle fibers using an open-source software, Fiji (aka ImageJ, Key Resources Table).[12] The Fiji software is widely used for image-processing and segmentation.[13] No programming

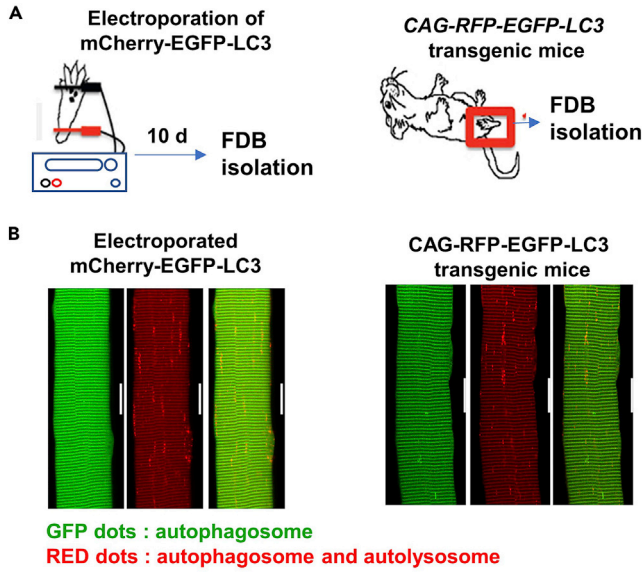

Figure 1. Use of mCherry-EGFP-LC3 as a fluorescent marker for autophagy execution in skeletal muscle

(A) 10 days after electroporation of the mCherry-EGFP-LC3 cDNA plasmid into the flexor digitorum brevis (FDB) of mice, individual FDB fibers were isolated for fluorescent imaging (left). Transgenic mice with expression of CAG-RFP-EGFP-LC3 were used for isolation of FDB muscle fibers (right).

(B) Aggregates of GFP fluorescence representing autophagosomes or RFP fluorescence representing autophagosomes and autolysosomes were observed in live FDB fibers 10 days after electroporation (left) or those derived from the CAG-RFP-EGFP-LC3 transgenic mice (right). The GFP puncta or RFP puncta appear on the background of striation patterns of baseline fluorescence due to non-vesicle-forming EGFP-LC3 expression on Z-line, as has been previously reported.[5] Scale bar indicates 20 μm.

knowledge is necessary to run Fiji Macros implemented in our protocol. Details of electroporation of FDB muscle in live mice[14] and isolation of individual skeletal muscle fibers from FDB muscle[15] are well-described previously.

Institutional permissions (if applicable)

Animal handling and surgical procedures were performed according to protocols approved by the Institutional Animal Care and Use Committee (IACUC) of The Ohio State University and were compliant with guidelines of the American Association for the Accreditation of Laboratory Animal Care. Before using this protocol, ensure that all animal studies are approved by IACUC or relevant local institutions.

Preparation of medium for animal treatment

Timing: 10 min

1. Preparing hyaluronidase solution.
   a. 2 mg/mL hyaluronidase dissolved in sterile saline solution.
   b. Mix gently.
2. Preparing colchicine stock solution.
   a. Colchicine was dissolved in sterile ddH_2O at a concentration of 4 mg/mL.
   b. Mix well and stored at −20°C.

Preparation of medium for FDB fiber isolation

Timing: 10 min

3. Preparing Tyrode solution:
   a. 140 mM NaCl, 5 mM KCl, 2.5 mM $CaCl_2$, 2 mM $MgCl_2$ and 10 mM HEPES in 1 L ddH_2O.
   b. Adjust PH to 7.2.
4. Preparing digestion solution:
   a. Add 2 mg of type I collagenase to 1 mL Tyrode solution.
   b. mix gently.

KEY RESOURCES TABLE

REAGENT or RESOURCE	SOURCE	IDENTIFIER
Chemicals, peptides, and recombinant proteins		
Hyaluronidase	Sigma-Aldrich	Cat# H4272
29-gauge needle	Exel International	Cat# EU12913
NaCl	Sigma-Aldrich	Cat# S9888
KCl	Sigma-Aldrich	Cat# 529552
$CaCl_2$	Sigma-Aldrich	Cat# 21115
$MgCl_2$	Sigma-Aldrich	Cat# M8266
HEPES	Sigma-Aldrich	Cat# H3375
Type I collagenase	Sigma-Aldrich	Cat# C5138
Glass-bottomed dishes	Nest Scientific	Cat# 801001
mCherry-EGFP-LC3	pEGFP-LC3 (Addgene 24920) was double digested with *Afe*I (blunt) and *BamH*I, yielding the 1.2 kb EGFP-LC3 segment. This segment was subcloned into pmCherry-C1 (Addgene 632524), which was opened by the digestion of *Sma*I (blunt) and *BamH*I.	
Experimental models: Organisms/strains		
C57Bl/6 mice, male, 17 weeks	The Jackson Laboratory	Cat# 000664
Software and algorithms		
Fiji ImageJ v1.53f	Schindelin et al.	https://imagej.net/software/fiji/
Macro: FFTmuscle.ijm	This paper	https://github.com/novashining/FFTmuscle
Example image folder – contains sample images to run the Macro	This paper	
Other		
Electroporation	Harvard Apparatus	ECM 830
Confocal Microscope	Zeiss	LSM 780

MATERIALS AND EQUIPMENT

Tyrode solution		
Reagent	Final concentration	Amount
NaCl	140 mM	8.18 g
KCl	5 mM	0.37 g
$CaCl_2$	2.5 mM	0.37 g
$MgCl_2$	2 mM	0.4 g
HEPES (1 M)	10 mM	10 mL
Total	N/A	1 L
Store at 4°C for six months.		

STEP-BY-STEP METHOD DETAILS

Preparation and isolation of FDB fiber

Timing: 10 days

In this step, we describe the steps to induce the overexpression of mCherry-EGFP-LC3 via electroporation in the mouse FDB fiber as well as the isolation of the FDB fiber for further evaluation.

1. Inject anesthetized mice with 10 μL of 2 mg/mL hyaluronidase dissolved in sterile saline at the ventral side of the hind paws using a 29-gauge needle.

   Note: Hyaluronidase digests components of the extracellular matrix to permit more efficient entry of plasmid into myofibers.

2. One hour later, inject 20 μL (2 mg/mL) mCherry-EGFP-LC3 plasmid DNA in autoclaved ddH_2O at the same site of hyaluronidase injection.
3. Electroporation of the muscle.
   a. Fifteen minutes later, place two electrodes (0.2 × 13 mm stainless steel acupuncture needles, Millennia, 210906) about 10 mm apart at the starting lines separating paw and toes.
   b. Apply twenty-five pulses of 100 V/cm electric field at 20 ms bursts with 1 s Burst interval under LV mode (ECM 830 Electro Square Porator, BTX, Holliston, MA).
4. On day 8, inject colchicine (0.4 mg/kg) intraperitoneally (IP) into the mice.

   Note: control mice receive an equal volume IP injection of autoclaved ddH_2O.

5. FDB fiber isolation.
   a. On day 10, surgically remove FDB muscles and place in Tyrode solution.
   b. Place the FDB muscle inside a tube with 1 mL digestion solution, then incubate for 40 min at 37°C in a shaking incubator.
   c. After collagenase treatment, dissociate the FDB fibers by several passages through a series of pipettes with decreasing diameter.[16]
   d. Plate the Fibers onto glass-bottomed dishes filled with Tyrode solution, and ready for imaging.

Confocal imaging

Timing: 1 h

6. Place the glass-bottomed dish with isolated FDB fibers on the dish holder of the microscope.

   Note: FDB fibers can be imaged up to 24 h post isolation[55], however we suggest that imaging within 2 h after the fiber isolation for best quality.

7. Confocal microscope setting and imaging:
   a. Image the Intact FDB fibers on a Zeiss 780 confocal microscope with 20× objective lens. A standard imaging setting was applied for the imaging. Using 488 nm Laser to excite EGFP and 594 nm Laser to excite mCherry.
   b. Use 2048*2048 scanning resolution to capture and save all images as original CZI files.

   Note: Microscopes from different companies may have their own file formats. Most of them can be read into Fiji-ImageJ automatically via an integrated Bio-Formats Importer.

Image processing and analysis

Timing: 20 min

The method below use a homemade ImageJ macro (FFTmuscle.ijm) to run batch processes on a single input folder of images. The program process and gener processed images and results were

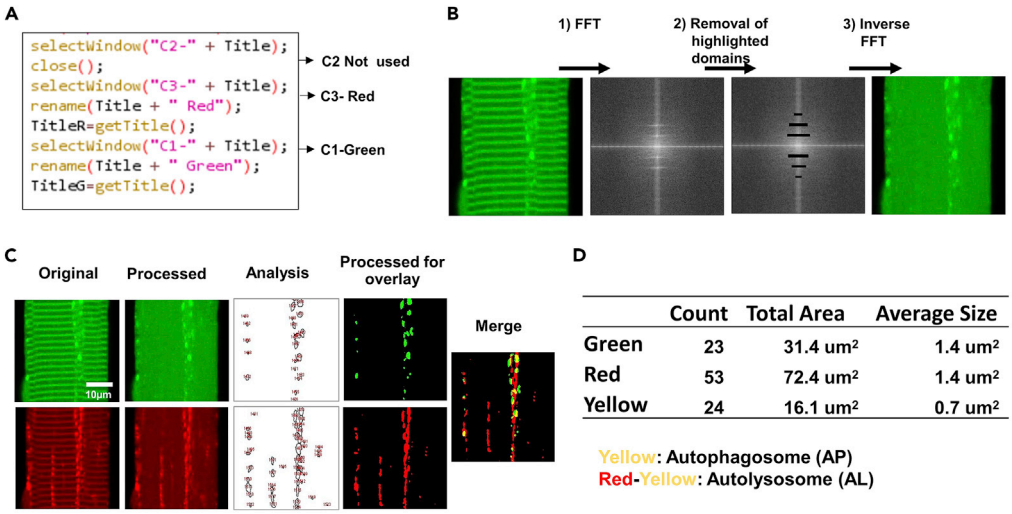

Figure 2. FFT processing to eliminate background fluorescence for quantification of autophagosomes and autolysosomes in FDB fibers

(A) ImageJ macro codes that users could change based on their specific imaging settings to select green or red channel.

(B) FFT is used to define patterns of basal fluorescence that are of repetitive nature (step 1), which is removed in step 2. In step 3, inverse FFT is used to reconstruct fluorescence image after subtraction of baseline fluorescence in single FDB muscle fiber.

(C) FFT image analyses of GFP (top) and RFP (bottom) for quantification of APs and ALs. Analysis were performed with processed fluorescence images of GFP or RFP after removal of the striation pattern. Processed images were merged to reveal the overlay pattern of GFP and RFP. GFP represents APs. RFP minus yellow puncta represents ALs.

(D) The number of green, red, or yellow puncta were quantified (count) and the area of fluorescence aggregates were calculated (total area), from which the average size was defined as total area/count.

output into a new folder within the user-selected directory (Figure 2). If using the user's own image sets, the directory structures may be different, and running the macro might need to be adapted accordingly. Entire images were used for analysis to avoid cherry-picking. The resolution needs to reach at least several pixels per punctum (for a given AP or AL), otherwise it would be difficult to distinguish them from random noise across the image.

8. Download the macro: FFTmuscle.ijm.
9. Open Fiji software.
10. Drag the macro file to the Fiji window.
11. A new macro window will be opened and all codes inside are available for further editing and optimization, e.g., selection of GREEN or RED channels.
12. Change of Macro Parameter:

⚠ CRITICAL: Since the experiments or imaging setting varies from the different muscle fibers, the parameter of the macro might need adjustment according to users' own experimental settings:

a. Channel assignments:
Lines 26–33, C1, C2, and C3 represent three split color channels of the image. In this case, C1 is green, C2 is transparent (not used), and C3 is red (Figure 2A).
b. Auto thresholding methods in lines 51 and 84:

Note: Maximum entropy thresholding can determine the optimal threshold value for image segmentation taking into consideration the probability distribution of target and background

composition without any prior information. Thus, it works well even with a variety of different expression levels of your target proteins (GFP or RFP).

c. Parameters to analyze EGFP- or mChery-positive particles in lines 66, 99, and 108:

Note: The size and circularity settings could be modified and optimized based on the users' preferences. Once it is set up, the setting should be used for the analysis of the whole set of images.

13. Click the "Run" button to start the macro.
    a. Select the desired input folder and output folder. Input folder contains all the images that users want to analyze. The output folder will store all processed images and results.
    b. Input the file suffix according to the file format (For example, type ".tif" for tif file format, ".czi" for Zeiss microscope file).
    c. Click "OK".
14. A new FFT image for the GREEN channel will be opened and a small window "waiting user" with an OK button will pop up.

⚠ CRITICAL: Do not click "OK" until step 16.

Note: The macro will automatically process the image and run FFT (the individual function can be found in "process > FFT"). FFT is an algorithm that computes the Discrete Fourier Transform (DFT) of a sequence, or its Inverse FFT (IFFT). Fourier transformation converts a signal from its original domain to a representation in the frequency domain. In this method, we used FFT to obtain the frequency domain image to eliminate the highly repetitive striation fluorescence pattern of skeletal muscle (Figure 2B).

15. FFT Based Image Processing (Figure 2B):
    a. Select the condensed segments above or below the center point of the FFT image that represent the repetitive striated pattern.
    b. Click the "delete" button on the keyboard to wipe the rectangle area to black. Make sure your foreground and background colors are set to White/Black in ImageJ.
    c. Repeat the above steps to delete other condensed segments above or below the center point.

Note: Since the pattern of the muscle, as well as the imaging settings, vary, automatically processing is not very reliable at this step. Thus, manual selection of the area is necessary. Although this step is not fully automatic and involves subjective input, the outcome of the analysis is still considered solid since only the repetitive pattern is eliminated and the puncta (AP or AL vesicles) will not be affected.

16. Once the desired segments have been deleted, click the "OK" button on the waiting user window to proceed to the quantification step. The macro will automatically perform inverse FFT to generate processed images containing condensed GFP-positive puncta representing different forms of AP or AL. The image is saved in the output folder. Figure 2C (*left panel*).
17. Repeat steps 7–9 for the RED channel. Figure 2C (*left panel*).
18. Once both GREEN and RED channel analyses are complete, a merged image of GFP and RFP is automatically generated as shown in Figure 2C (*right panel*).
19. A new window will open showing the total count and total area of GFP and RFP positive puncta, as shown in Figure 2D. The average size for the given frame represents the total area/count.
20. After finishing the current image, the macro will start to process the next image (of a different FDB muscle fiber) and repeat until all the images in the input folder are all processed and analyzed.
21. Save the summary results and the file can be opened in Excel for further statistical evaluation.

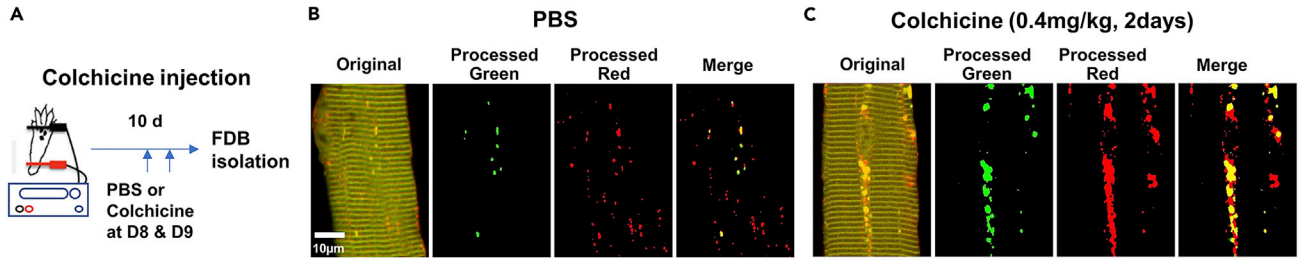

Figure 3. Colchicine treatment inhibits execution of autolysosome in FDB fiber

(A) Colchicine (0.4 mg/kg, intraperitoneal) was administered to mice at Day 8 and Day 9 after electroporation of mCherry-EGFP-LC3 into the FDB muscle. PBS was injected into mice as control.

(B) FFT processing of GFP and RFP in FDB fibers following PBS injection.

(C) FFT processing of GFP and RFP in FDB fibers following colchicine treatment demonstrates the increased pattern of yellow fluorescence as expected with the inhibition of lysosome fusion with AP.

EXPECTED OUTCOMES

To study the dynamic autophagy in isolated muscle fibers, our protocol overcomes the challenges during analysis involving manual handling and user-based decisions. This semi-automated computational approach improves objectivity by minimizing bias associated with manual image processing for quantification of AP and AL. With this protocol, GFP^+/RFP^+ or GFP^-/RFP^+ vesicles can be reliably quantified in individual isolated FDB muscle fibers. As demonstrated in current study, our established protocol allowed a quantitative evaluation of autophagy flux in skeletal muscle with the application of colchicine, a compound known to block autophagosome degradation by inhibition of fusion of Autophagosomes to lysosomes in skeletal muscle.[17] As shown in Figure 3, treatment of mice with colchicine results in an increased pattern of yellow fluorescence, demonstrating the inhibitory effect of colchicine on blocking AP degradation.

QUANTIFICATION AND STATISTICAL ANALYSIS

The summary data can be exported to most of the commonly used data analysis software such as Excel or GraphPad Prism. The summary files may contain redundant columns, which are unnecessary for analyses. Generally, the columns relating to counts, total area, and average size are the only necessary columns (Figure 2D). Statistical analysis can be performed on the absolute or relative measurements as required.

LIMITATIONS

This method used electroporation for *in vivo* gene transfection in skeletal muscle. The electroporation procedure can induce stress to the local tissue, which may alter the autophagy activity locally. Although the imaging of AP/AL was performed 10 days after the electroporation to minimize the potential effect of the electroporation, the potential remaining damage may not be completely ruled out. Biochemical analysis of autophagy flux should be also included to arrive a final conclusion.

Multiple compounds have been used to block the autophagosome degradation in order to evaluate autophagy flux in cultured cells or live animals, such as colchicine, bafilomycin A1 or chloroquine, etc. In the current study, we followed a well-established protocol[17] to evaluate the autophagy flux in the skeletal muscle of live mice, using colchicine. In the study of Ju et al., colchicine showed a more potent effect in blocking autophagosome degradation when compared with chloroquine (colchicine: 0.4 mg/kg/day vs chloroquine 50 mg/kg/day). However, we would encourage readers to explore the efficacy of other compounds as inhibitors of autophagosome degradation when developing their own protocols for evaluating autophagy flux in skeletal muscle of adult mice by considering some parameters, such as the dosage (specificity), onset-time, toxicity for live animals, and cost, etc.

This protocol is optimized for quantifying the distribution of RED, GREEN, and YELLOW positive vesicles and their size in isolated skeletal muscle fibers, which expresses mCherry-EGFP-LC3 from 2D fluorescent images. The Green only signal theologically should not exist, but it has been commonly observed in cells with overexpression of mCherry-EGFP-LC3,[4,18] and it should be considered as the artifact signal. We recommend the Green only signal should not be grouped into either AP or AL during analysis.

The automated segmentation was designed for differentiating the fluorescent puncta (AP and AL) from the striation background in a single muscle fiber. The resolution to distinguish individual puncta could be limited if too many puncta are aggregated together. However, this will not affect the total area quantification. Additionally, atypical morphologies of muscle fibers, i.e., blebbing, twisting, or disorganized striation pattern, etc. may amplify the artifacts during the imaging processing. Thus, to limit the potential artifacts, images should be taken from undamaged muscle fibers showing clear Z-line striation patterns.

TROUBLESHOOTING

Problem 1

The condition of isolated muscle fiber is poor.

Potential solution

The condition of the isolated muscle fibers largely depends on the digestion condition. The key parameters could be the duration of the digestion. The activity of collagenase may vary between different venders or batches. Preliminary tests might be necessary for establishing an optimal condition for muscle fiber digestion.

Problem 2

Unexpected positive puncta after image processing.

Potential solution

The false-positive puncta usually result from damaged FDB fibers. Avoiding damaged fibers could reduce the false positive puncta.

Problem 3

Too many GREEN positive puncta are detected when compared with RED positive puncta.

Potential solution

It could be caused by setting the green signal too high or red signal too low during the imaging acquisition. The fluorescent intensity should be balanced between the Green and Red signals.

Problem 4

The quantification generated false positive counting on a FDB fiber without any appearance of fluorescent punctum.

Potential solution

The use of auto-threshold method requires at least one or several positive puncta in the muscle fiber in order to distinguish the signal from the background and allow the program to function normally. Users should manually record 0 for the fibers without any punctum.

RESOURCE AVAILABILITY

Lead contact

Further information and requests for resources and reagents should be directed to and will be fulfilled by the lead contact Jae-kyun Ko (jae-kyun.ko@osumc.edu).

Materials availability

The material generated in this study is available upon request from the lead contact.

Data and code availability

The codes used in the study are available on GitHub. Any additional information required to reanalyze the data is available from the lead contact upon request. Readers could contact Xinyu Zhou (Xinyu.Zhou@osumc.edu) for technical support.

ACKNOWLEDGMENTS

This study was supported by grants from the National Institutes of Health to J.M. (R01AG071676 and R01HL157215) and J.Z. (R01NS105621 and R01HL138570).

AUTHOR CONTRIBUTIONS

Conceptualization, Methodology, X.Z., J.H.C., J.M.; Writing – Original Draft, J.H.C., X.Z.; Writing – Review & Editing, all authors; Funding Acquisition and Supervision, J.M., J.Z.

DECLARATION OF INTERESTS

The authors declare no competing interests.

REFERENCES

1. Kabeya, Y., Mizushima, N., Ueno, T., Yamamoto, A., Kirisako, T., Noda, T., Kominami, E., Ohsumi, Y., and Yoshimori, T. (2000). LC3, a mammalian homologue of yeast Apg8p, is localized in autophagosome membranes after processing. EMBO J. *19*, 5720–5728. https://doi.org/10.1093/emboj/19.21.5720.

2. Shaner, N.C., Steinbach, P.A., and Tsien, R.Y. (2005). A guide to choosing fluorescent proteins. Nat. Methods *2*, 905–909. https://doi.org/10.1038/nmeth819.

3. Shaner, N.C., Campbell, R.E., Steinbach, P.A., Giepmans, B.N.G., Palmer, A.E., and Tsien, R.Y. (2004). Improved monomeric red, orange and yellow fluorescent proteins derived from Discosoma sp. red fluorescent protein. Nat. Biotechnol. *22*, 1567–1572. https://doi.org/10.1038/nbt1037.

4. Pankiv, S., Clausen, T.H., Lamark, T., Brech, A., Bruun, J.A., Outzen, H., Øvervatn, A., Bjørkøy, G., and Johansen, T. (2007). p62/SQSTM1 binds directly to Atg8/LC3 to facilitate degradation of ubiquitinated protein aggregates by autophagy. J. Biol. Chem. *282*, 24131–24145. https://doi.org/10.1074/jbc.M702824200.

5. Xiao, Y., Ma, C., Yi, J., Wu, S., Luo, G., Xu, X., Lin, P.H., Sun, J., and Zhou, J. (2015). Suppressed autophagy flux in skeletal muscle of an amyotrophic lateral sclerosis mouse model during disease progression. Physiol. Rep. *3*, e12271. https://doi.org/10.14814/phy2.12271.

6. Tjondrokoesoemo, A., Park, K.H., Ferrante, C., Komazaki, S., Lesniak, S., Brotto, M., Ko, J.K., Zhou, J., Weisleder, N., and Ma, J. (2011). Disrupted membrane structure and intracellular Ca(2)(+) signaling in adult skeletal muscle with acute knockdown of Bin1. PLoS One *6*, e25740. https://doi.org/10.1371/journal.pone.0025740.

7. Xiao, Y., Karam, C., Yi, J., Zhang, L., Li, X., Yoon, D., Wang, H., Dhakal, K., Ramlow, P., Yu, T., et al. (2018). ROS-related mitochondrial dysfunction in skeletal muscle of an ALS mouse model during the disease progression. Pharmacol. Res. *138*, 25–36. https://doi.org/10.1016/j.phrs.2018.09.008.

8. Yi, J., Ma, C., Li, Y., Weisleder, N., Ríos, E., Ma, J., and Zhou, J. (2011). Mitochondrial calcium uptake regulates rapid calcium transients in skeletal muscle during excitation-contraction (E-C) coupling. J. Biol. Chem. *286*, 32436–32443. https://doi.org/10.1074/jbc.M110.217711.

9. Pouvreau, S., Royer, L., Yi, J., Brum, G., Meissner, G., Ríos, E., and Zhou, J. (2007). Ca(2+) sparks operated by membrane depolarization require isoform 3 ryanodine receptor channels in skeletal muscle. Proc. Natl. Acad. Sci. USA *104*, 5235–5240. https://doi.org/10.1073/pnas.0700748104.

10. Li, L., Wang, Z.V., Hill, J.A., and Lin, F. (2014). New autophagy reporter mice reveal dynamics of proximal tubular autophagy. J. Am. Soc. Nephrol. *25*, 305–315. https://doi.org/10.1681/ASN.2013040374.

11. Lin, F., Wang, Z.V., and Hill, J.A. (2014). Seeing is believing: dynamic changes in renal epithelial autophagy during injury and repair. Autophagy *10*, 691–693. https://doi.org/10.4161/auto.27749.

12. Schindelin, J., Arganda-Carreras, I., Frise, E., Kaynig, V., Longair, M., Pietzsch, T., Preibisch, S., Rueden, C., Saalfeld, S., Schmid, B., et al. (2012). Fiji: an open-source platform for biological-image analysis. Nat. Methods *9*, 676–682. https://doi.org/10.1038/nmeth.2019.

13. Dobson, E.T.A., Cimini, B., Klemm, A.H., Wählby, C., Carpenter, A.E., and Eliceiri, K.W. (2021). ImageJ and CellProfiler: complements in open-source bioimage analysis. Curr. Protoc. *1*, e89. https://doi.org/10.1002/cpz1.89.

14. Cai, C., Masumiya, H., Weisleder, N., Matsuda, N., Nishi, M., Hwang, M., Ko, J.K., Lin, P., Thornton, A., Zhao, X., et al. (2009). MG53 nucleates assembly of cell membrane repair machinery. Nat. Cell Biol. *11*, 56–64. https://doi.org/10.1038/ncb1812.

15. Park, K.H., Weisleder, N., Zhou, J., Gumpper, K., Zhou, X., Duann, P., Ma, J., and Lin, P.H. (2014). Assessment of calcium sparks in intact skeletal muscle fibers. J. Vis. Exp. e50898. https://doi.org/10.3791/50898.

16. Weisleder, N., Brotto, M., Komazaki, S., Pan, Z., Zhao, X., Nosek, T., Parness, J., Takeshima, H., and Ma, J. (2006). Muscle aging is associated with compromised Ca2+ spark signaling and segregated intracellular Ca2+ release. J. Cell Biol. *174*, 639–645. https://doi.org/10.1083/jcb.200604166.

17. Ju, J.S., Varadhachary, A.S., Miller, S.E., and Weihl, C.C. (2010). Quantitation of "autophagic flux" in mature skeletal muscle. Autophagy *6*, 929–935. https://doi.org/10.4161/auto.6.7.12785.

18. Kondratskyi, A., Kondratska, K., Vanden Abeele, F., Gordienko, D., Dubois, C., Toillon, R.A., Slomianny, C., Lemière, S., Delcourt, P., Dewailly, E., et al. (2017). Ferroquine, the next generation antimalarial drug, has antitumor activity. Sci. Rep. *7*, 15896. https://doi.org/10.1038/s41598-017-16154-2.